

Article

# Low-Cost Solar Irradiance Sensing for PV Systems

Miguel Carrasco <sup>1</sup>, Antonino Laudani <sup>2</sup>, Gabriele Maria Lozito <sup>2,\*</sup>, Fernando Mancilla-David <sup>1</sup>, Francesco Riganti Fulginei <sup>2</sup>  and Alessandro Salvini <sup>2</sup>

<sup>1</sup> Department of Electrical Engineering, University of Colorado Denver, Denver, CO 80217, USA; miguel.carrasco.lopez@gmail.com (M.C.); fernando.mancilla-david@ucdenver.edu (F.M.-D.)

<sup>2</sup> Department of Engineering, Università degli Studi Roma Tre, 00149 Roma, Italy; antonino.laudani@uniroma3.it (A.L.); francesco.rigantifulginei@uniroma3.it (F.R.F.); alessandro.salvini@uniroma3.it (A.S.)

\* Correspondence: gabriemaria.lozito@uniroma3.it

Academic Editor: Enrico Sciubba

Received: 18 January 2017; Accepted: 10 July 2017; Published: 14 July 2017

**Abstract:** Determination of solar irradiance is a critical asset to ensure efficient working conditions for a photovoltaic (PV) system. This work analyze the feasibility of assessing solar irradiance on a PV device assuming the knowledge of the device temperature and the voltage/current operating point. This work proposes an approach based on a manipulation of the analytic expressions found in the reduced form of the “single diode” circuit model for a silicon PV device. The approach was validated through different practical experiments, and the results obtained are comparable to the ones of a commercial instrument for irradiance sensing. The ease of construction and the reduced costs involved make a device based on the proposed approach suitable for large-scale integration in a PV plant.

**Keywords:** parameter estimation; photovoltaic power systems; renewable energy; solar radiation

---

## 1. Introduction

Assessment of solar irradiance ( $G$ ) is critical to ensure the correct and efficient operation of a system based on photovoltaic technology (PV). This is especially true for power applications where the optimal work point is determined by a Maximum Power Point Tracking (MPPT) algorithm, since the optimal operating point drastically changes according to environmental conditions such as cell temperature ( $T$ ) and irradiance. The determination of  $T$  is trivial, though any temperature determined by an external thermometer should take into account a correction factor to express the junction temperature (i.e., the one that really affects the  $I$ - $V$  characteristic). On the other hand, sensing solar irradiance is rather difficult and requires expensive instruments. A periodic calibration is required for those instruments. Even if an approximate value for irradiance might be obtained by direct interrogation of the nearest meteorological station, this is rather unpractical. First, a fast online connection to the station should be implemented, which is a difficult requirement to meet in rural areas. Second, the meteorological measurement could differ significantly from the actual irradiance on the PV plant. The critical nature of the determination of  $G$  is evident if we consider large power plants with problems of partial shadowing. In this case, a complete knowledge of the irradiance profile in the plant can help to increase the efficiency of the power extraction process [1]. Indeed, the sensed irradiance should be directly illuminating the PV module (i.e., the one relevant for energy production). Thus, the operator must place any sensor geometrically parallel to the panel itself. Direct sensing of irradiance on each PV module can be a rather unpractical solution, and for this reason, several authors propose alternative approaches in the literature [1–8]. In particular, some of these approaches focus on models representing the PV array. Some authors propose to estimate the irradiance by

approximating the equations describing the PV device model [2–4], or by measuring either open circuit voltage or short circuit current [5–7]. In [8], the authors generalize the implicit unknown relationship between irradiance and operating point of a PV device by means of an artificial neural network (ANN) implemented on an embedded MCU (microcontroller unit). The approach proposed in [8] is very interesting due to the computational advantage of using an ANN in a low-resource environment such as a MCU. In particular, the board used in [8] mounts a low-end microchip device featuring a web server on an ethernet protocol, which is very interesting for distributed irradiance measuring. Since the solar irradiance is correlated to the Maximum Power Point (MPP), the neural approach was also used to determine the optimal voltage  $v_{mpp}$  using a simple feed-forward ANN on low-end MCUs [9] and high-end Advanced Reduced Instruction Set Computer Machine (ARM) devices [10,11]. Addressing this problem through an ANN is effective and among the best solutions in terms of accuracy and low-cost strategies. Indeed, this methodology has the limitation of a classic black-box approach, which is the absence of an explicit formulation for the problem. This makes analyzing the performance of the predictor beyond mere error accuracy (e.g., sensibility analysis) impossible. The scope of this work is to explore the feasibility of an alternative approach for indirect solar irradiance sensing. The approach proposed in this work starts from an analytic manipulation of the equations describing a very versatile and known circuit model for a PV device. Literature refers to this model as “one diode model” or “five parameters model”. Assuming this model is identified with accuracy, the irradiance can be computed by knowledge of the device operating voltage/current point (V,I) and the actual temperature T of the cell. The paper is structured as follows: In Section 2, we present the reasons behind this study and the novelties introduced with respect to the state of the art. In Section 3, we describe the equivalent one-diode circuit model for a PV device. In Section 4, we discuss an analytic approach to estimate solar irradiance (based on the model described in Section 3). In Section 5, we describe an experimental implementation of the approach, and we validate it in two different scenarios against a commercial solar irradiance sensor (as reference, in the same section, we report a validation against an ANN approach). In Section 6, we discuss possible uses of the obtained research results in the form of potential applications. Final remarks close the paper.

## 2. The Problem of Sensing Solar Irradiance

Solar irradiance is the power per unit area ( $\text{W/m}^2$ ), in form of electromagnetic radiation, received by the Sun. For applications of electric energy generation from photovoltaic conversion, solar irradiance is measured on the surface of the converting device (e.g., a PV panel). This quantity is directly related to the overall insolation, but is strongly influenced by relative orientation of the device with respect to the sunrays, occlusions by clouds, refraction by nearby surfaces, absorption by air humidity, and reflectance by the panel glass surface. All these factors are very difficult to take into account in a solar irradiance estimation. For this reason, a common approach is to measure this quantity by means of sensors directly placed near the device under monitoring. The classic instrument used for irradiance measurement is the pyranometer.

Knowledge of solar irradiance is very important for several scenarios involving energy generation from PV conversion, in particular:

- Maximum Power Point Tracking.
- Power plant efficiency monitoring.
- Reconfiguration of distributed PV plants to manage partial shading problems.
- Monitoring and maintenance for panels’ degradation over time.
- Energy market arbitrage.
- Prediction of power flows for smart grid configuration.

Unfortunately, measurement of solar irradiance on a PV panel by means of a pyranometer is an expensive and unpractical solution. This is due to different reasons. First, the pyranometer is a costly instrument that needs periodic calibration. Second, the spectral response of the pyranometer

might be different from the one of the PV device under monitoring. Third, since the geometrical inclination between sensor and sunrays influences  $G$  heavily, a rigid mechanical structure holding the pyranometer close and parallel to the PV panel is required. In this work, we propose a solar irradiance measurement procedure that solves all the aforementioned issues.

### 3. The “One Diode” Model and Its Generalization for a PV Array

A very common circuit model used both in literature and industrial application to represent silicon based PV device is the one known as “One diode” model, or “Five parameters” model. This model (for a single cell) is composed by an independent current generator, an antiparallel diode, a series resistor and a shunt resistor. The same model can be generalized for a generic PV array composed by  $N_S$  series cells and  $N_P$  parallel cells through suitable manipulation of the single cell circuital component values [12]. This allows creating the circuital representation for the whole array, shown in Figure 1. The IV characteristic of such circuit, expressing the array’s current ( $i_{pv}$ ) and voltage ( $v_{pv}$ ) is the following:

$$i_{pv} = N_p I_{irr} - N_p I_0 \left[ \exp \left( \frac{q(v_{pv} + i_{pv} N_S R_S / N_P)}{N_S n k T} \right) - 1 \right] - \frac{v_{pv} + i_{pv} N_S R_S / N_P}{N_S R_P / N_P} \quad (1)$$

The constants appearing in the previous equations are the following:  $q = 1.602 \times 10^{-19}$  C is the electron charge,  $k = 1.3806503 \times 10^{-23}$  J/K is the Boltzmann constant and  $n$  is the ideality factor of the diode.

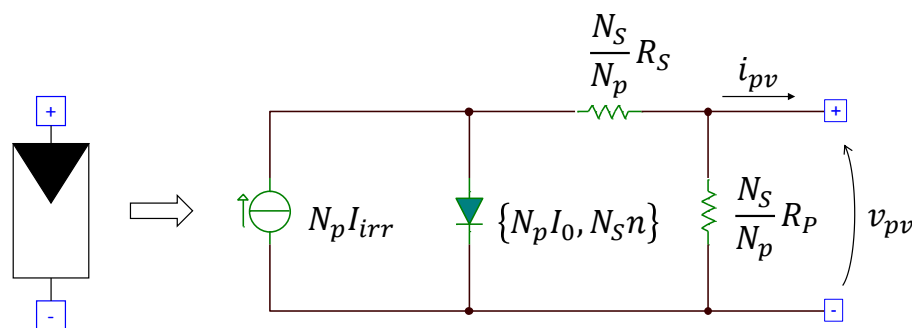


**Figure 1.** One-diode model for a photovoltaic device composed by  $N_S$  series cells and  $N_P$  parallel cells.

The adaptation of the circuit parameters for an array of cells is the following. The array current generator has value  $N_p I_{irr}$ , where  $I_{irr}$  is the current generator of the single cell. The array inverse saturation current is  $N_p I_0$ , the series resistance is  $N_S / N_P R_S$ , the shunt resistance is  $N_S / N_P R_P$  and the ideality factor of the diode is  $N_S n$ . The quantities  $I_0$ ,  $R_S$ ,  $R_P$  and  $n$  are respectively inverse saturation current, series resistance, shunt resistance and diode ideality factor for the single cell. Each circuital parameter is a function of the irradiance  $G$  and the cell temperature  $T$ . This dependence is usually expressed in terms of some constant reference values estimated at standard reference conditions (SRC, equal to  $G_{ref} = 1000$  W/m<sup>2</sup> and  $T_{ref} = 298.5$  K) denoted as  $I_{irr,ref}$ ,  $I_{0,ref}$ ,  $R_{Pref}$ ,  $R_{Sref}$ ,  $n_{ref}$ . The equations expressing the parameters dependence are the ones from (2) to (6). In (2) the term  $\alpha_T$  is a coefficient expressing the rate of change for the short-circuit current against the absolute temperature [13].

$$I_{irr} = \frac{G}{G_{ref}} \left( I_{irr,ref} + \alpha_T (T - T_{ref}) \right) \quad (2)$$

$$I_0 = I_{0,ref} \left( \frac{T}{T_{ref}} \right)^3 \exp \left[ \frac{E_{g,ref}}{kT_{ref}} - \frac{E_g}{kT} \right] \quad (3)$$

$$R_P = R_{P,ref} \left( \frac{G_{ref}}{G} \right) \quad (4)$$

$$R_S = R_{S,ref} \quad (5)$$

$$n = n_{ref} \quad (6)$$

The term  $E_g$  in (3) is the energy, expressed in eV, for the silicon bandgap. We used two different interpolating expressions for the temperature dependence of this parameter, in order to verify potential differences in the results. These formulae are adopted commonly in literature. The first expression is due to Varshni [14]

$$E_g(T) = E_{g0} - \frac{AT^2}{T + B} \quad (7)$$

where the parameters  $E_{g0}$ ,  $A$  and  $B$  assume, for silicon, the values  $1.17$ ,  $4.73 \times 10^{-4}$  and  $636$  respectively (values for different types of materials can be found in [14] and in [15]). Another simple linear-interpolating expression was proposed in [13], yielding:

$$E_g = E_{g,T_{ref}} \left( 1 - 0.0002677 (T - T_{ref}) \right) \quad (8)$$

The cell parameters at SRC are specific for the PV device. Several procedures can be used to extract those parameters either from experimental I-V curves [16] or from the manufacturer datasheet [17,18]. Since the sensing approach proposed in this work is based directly on model equations, an accurate procedure able to identify the model from experimental data such as the one shown in [16] is of paramount importance for the methodology implementation.

#### 4. Closed-Form Expression for Solar Irradiance

The closed-form expression for solar irradiance is obtained by algebraic manipulation of the voltage-current characteristic of the model. Starting from (1), we can write explicitly the parameters that depend on irradiance (i.e.,  $R_P$  and  $I_{irr}$ ), getting:

$$\begin{aligned} i_{pv} &= \frac{G}{G_{ref}} N_P \left( I_{irr,ref} + \alpha_T (T - T_{ref}) \right) - N_P I_0 \left[ \exp \left( \frac{q \left( v_{pv} + \frac{i_{pv} N_S R_{S,ref}}{N_P} \right)}{N_S n k T} \right) - 1 \right] \\ &\quad - \frac{v_{pv} + i_{pv} N_S R_{S,ref} / N_P}{N_S R_{P,ref} / N_P \left( \frac{G_{ref}}{G} \right)} \end{aligned} \quad (9)$$

We can manipulate this expression to obtain:

$$\begin{aligned} \frac{G}{G_{ref}} \left( N_P I_{irr,ref} + N_P \alpha_T (T - T_{ref}) - \frac{v_{pv} + i_{pv} N_S R_{S,ref} / N_P}{N_S R_{P,ref} / N_P} \right) \\ = i_{pv} + N_P I_0 \left[ \exp \left( \frac{v_{pv} + i_{pv} N_S R_{S,ref} / N_P}{N_S n k T} \right) - 1 \right] \end{aligned} \quad (10)$$

Then, by expressing the temperature dependence of  $I_0$ , we obtain:

$$G = \frac{i_{pv} + C_6 T^3 \exp \left( C_7 - \frac{C_8}{T} + \frac{C_9 T}{T + C_{10}} \right)}{C_4 + C_5 T - C_3 (v_{pv} + C_2 i_{pv})} \left[ \exp \left( \frac{C_1 (v_{pv} + C_2 i_{pv})}{T} \right) - 1 \right] \quad (11)$$

Given the following constants:

$$\begin{aligned}
 C_1 &= \frac{q}{N_S n k} \quad C_2 = \frac{N_S R_{S,ref}}{N_P} \quad C_3 = \frac{N_P}{N_S R_{P,ref} G_{ref}} \\
 C_4 &= \frac{N_P}{G_{ref}} \left( I_{irr,ref} - \alpha T_{ref} \right) \quad C_5 = \frac{N_P}{G_{ref}} \alpha \quad C_6 = \frac{N_P I_{0,ref}}{T_{ref}^3} \\
 C_7 &= \frac{E_{g,ref} \times 1.602 \times 10^{-19}}{k T_{ref}} \quad C_8 = \frac{1.17 \times 1.602 \times 10^{-19}}{k} \\
 C_9 &= \frac{4.73 \times 10^{-4} \times 1.602 \times 10^{-19}}{k} \quad C_{10} = 636
 \end{aligned} \tag{12}$$

By using (9), it is possible to compute the irradiance directly as a function of the temperature  $T$ , the current  $i_{pv}$  and the voltage  $v_{pv}$  of the cell. The temperature can be measured by means of a temperature sensor mounted directly on the back of the module (frontal mounting is not used to avoid shadowing). The difference between the front and back temperature is usually below few degrees for a rapid change of meteorological conditions. This bias error can be easily corrected. We propose to assess the magnitude of the error due to a temperature bias experimentally. Consider the Mean Percentage Error (MPE) defined as:

$$MPE(\Delta T) = \frac{100\%}{n} \sum_{i=1}^n \frac{G(V_i, I_i, T_i) - G(V_i, I_i, T_i + \Delta T)}{G(T_i)} \tag{13}$$

where  $G$  is the irradiance computed from (11), the operating point  $(V_i, I_i, T_i)$  is the  $i$ -th Voltage/Current/Temperature of a suitable  $n$ -points dataset and  $\Delta T$  is a temperature bias. The MPE as a function of  $\Delta T$  for an experimental dataset composed by 424 (V,I,T) triplets is shown in Figure 2.

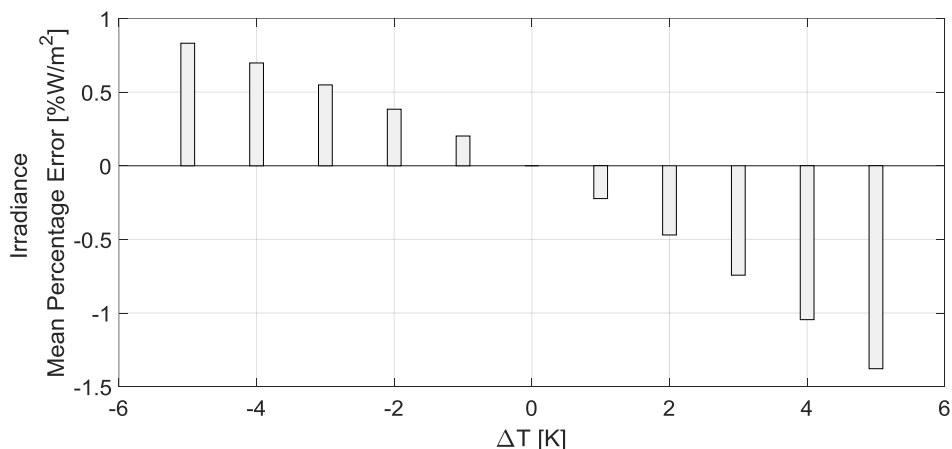


**Figure 2.** MPE over a variable dataset of experimental data for a bias error on temperature.

As can be seen from Figure 2, the error is lower than 1.5% for variations of  $\pm 5$  K. This error is very small, and can be corrected either by adjusting a measurement bias compensation, or can be simply taken into account in the measurement uncertainty. Traditional measurement approaches may require a forced short-circuit or open-circuit condition on the cell [6,7,19,20], using iterative algorithms [6,21] or using approximations or fitted data [2,4,8]. It should be noted that the computed value of  $G$  is the actual insolation for the panels, and for this reason, is the relevant parameter to be used in MPPT algorithms.

## 5. Experimental Setup and Validation

The proposed approach for irradiance sensing was implemented in an experimental setup to compare it against a commercial device for solar irradiance measurement. This setup has already been used in other works by the same authors to approaches for solar irradiance assessment [8]. The device

chosen was a silicon pyranometer model Silicon Pyranometer (SP) Lite 2 from Kipp & Zonen. This instrument is able to measure the irradiance with 10 s intervals. The sensor proposed in this work was developed on a microcontroller unit (MCU) board. The chosen device was a UNO by Arduino. The experimental setup involved both power-producing devices and smaller PV arrays. The first experiment involved eight monocrystalline PV cells connected in series, a 3.4 V/12 mW array model KXOB22-01X8 by IXYS (Milpitas, CA, USA). In this case, the goal was to verify the feasibility of using this approach in creating a stand-alone measurement instrument. The second experiment featured the direct irradiance measuring on a 17.4 V/87 W PV panel from Kyocera (model KC85TS), aiming at demonstrating the capability of this approach of estimating irradiance for a PV power plant. Both scenarios sees the PV devices loaded with a resistor of known value, to avoid the necessity of including a current sensor (the current is extrapolated by the microcontroller though direct application of Ohm's law). This simplifies the setup greatly and is very important to create a simple and portable stand-alone measurement instrument. The resistor value was chosen according to the I-V characteristic of the device, to ensure that, at SRC, the device would work at its MPP. To measure the temperature, a digital thermometer by Maxim Integrated, model DS18B20, was used.

This device communicates by means of 1-Wire protocol. The thermometer was mounted on the back of the array by means of a thermal paste layer. A schematic representation of the setup can be seen in Figure 3. Measurements were acquired every 800 ms and data was compared against the pyranometer. Atmospheric conditions featured an overcast day with rapidly moving clouds, and thus, rapidly varying levels of irradiance. The experiments were conducted on the University of Colorado Denver campus, located in downtown Denver (CO). The setup for the first experiment (IXYS cell) is shown in Figure 4 and the setup for the second experiment (Kyocera panel) is shown in Figure 5. As can be seen in both figures, a rigid structure holds the pyranometer and the sensor/panel geometrically parallel so that the solar irradiance is the same for the two devices.

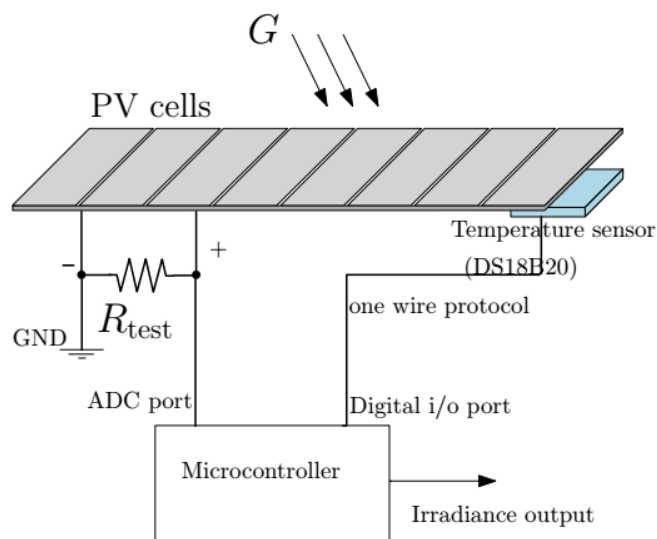


**Figure 3.** Setup as a single device irradiance sensor.

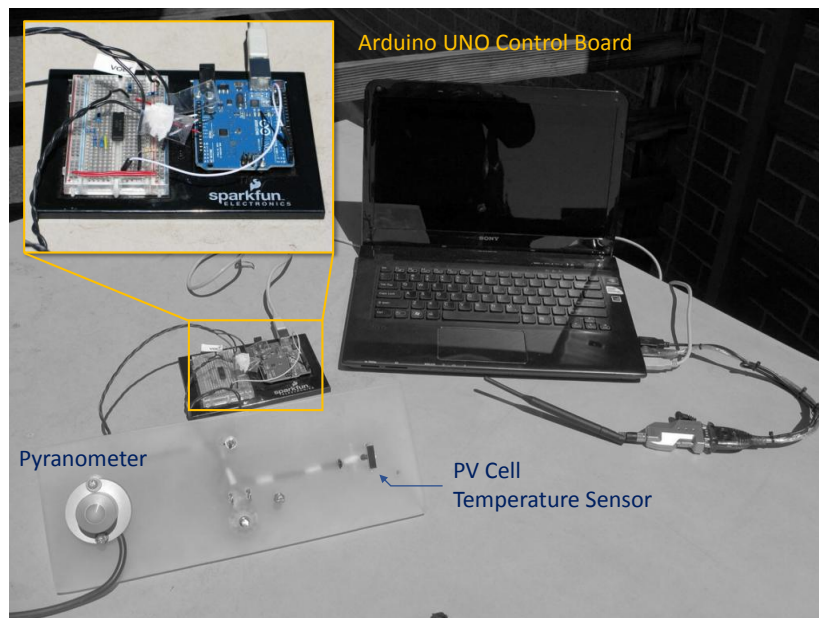


**Figure 4.** Experimental setup for validation of the irradiance sensing approach as a stand-alone measurement device. The reference pyranometer is geometrically parallel to the measurement PV cell. The temperature sensor is mounted on the back of the PV cell.

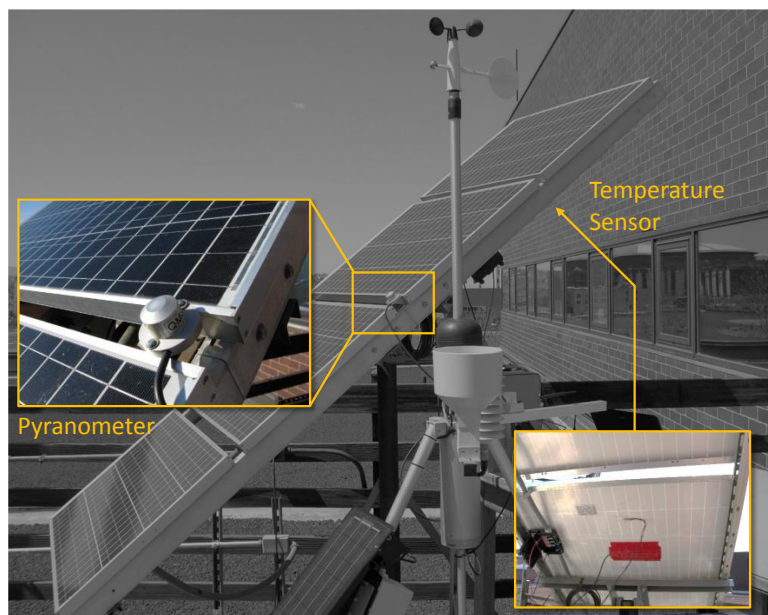


**Figure 5.** Experimental setup for validation of the irradiance sensing approach on a power producing PV panel. The reference pyranometer is rigidly mounted on the panel itself. The temperature sensor was mounted on the back of the panel.

### 5.1. Low Power PV Array

The first part of this test was performed on a low-cost, low-power 3.4 V/12 mW array model KXOB22-01X8 by IXYS. The final goal of this experiment was to assess the accuracy of a sensor based on the irradiance expression proposed. To investigate the parameters influence on the irradiance, different expressions for the silicon energy band gap were used. Moreover, the effect of neglecting the shunt resistance  $R_p$  was investigated.

As stated before, the approach needs an identified model to work. The model was easily identified from datasheet values. Concerning the band gap, both Equations (7) and (8) were used. In both cases, the five parameters were very similar, as can be seen in Table 1. Measurements were taken on 7 May 2014 on the roof of the North Classroom building at the University of Colorado Denver campus. The weather was partially overcast and wind speed ensured a rapid movement of the clouds, causing rapid variations of the solar irradiance. The figure of merit chosen to assess the accuracy of the method is the Root Mean Square (RMS) normalized to the mean of the instrument readings. For the two models, results shows an error of approximately 1.5%, which is a satisfactory result. The time dependent irradiance measured by the pyranometer and computed by the MCU using (9) can be seen in Figure 6. Concerning the investigation of the irradiance dependence against the shunt resistance, an alternate expression was used to compute the irradiance:

$$G = G_{ref} \frac{i_{pv} + N_p I_{0,ref} \left( \frac{T}{T_{ref}} \right)^3 e^{K_1 K_2} + \left( \frac{v_{pv} + i_{pv} N_S R_S / N_p}{N_S R_p / N_p} \right)} {N_p [I_{irr,ref} + \alpha_T (T - T_{ref})]} \quad (14)$$

$$K_1 = \frac{E_{g,ref}}{kT_{ref}} - \frac{E_g}{kT} \quad (15)$$

$$K_2 = \exp \left( \frac{q \left( v_{pv} + \frac{i_{pv} N_S R_S}{N_p} \right)}{N_S n k T} \right) - 1 \quad (16)$$

This expression is very similar to (9) but in this case a constant parameter for the shunt resistance,  $R_p$  (i.e., the shunt resistance is the same measured at SRC), was considered. For this simplified model, the error rises up to 7%. This underlines the relevance for the irradiance dependence of the  $R_p$  parameter.

**Table 1.** Circuit model parameters for a low-power PV array KXOB22-01X8 according to alternative band gap energy laws.

Parameter	$E_g$ Given by Equation (7)	$E_g$ Given by Equation (8)
$I_{irr,ref}$ [mA]	4.55047	4.55113
$I_{0,ref}$ [fA]	$7.66111 \times 10^{-7}$	$5.59818 \times 10^{-7}$
$R'_S [\Omega]$	249.28221	249.76964
$R'_P [k\Omega]$	7.28921	7.27189
$n$	0.53078	0.52695

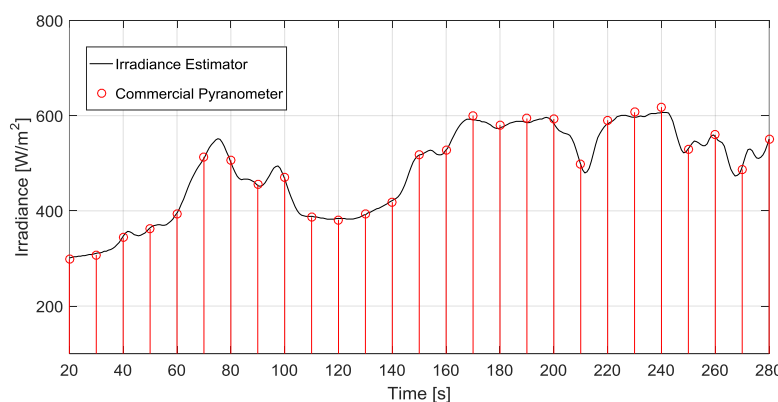


**Figure 6.** Irradiance profile predicted using a commercial pyranometer (red markers) and the proposed sensor on a low power PV array. RMS is about 1.5%.

## 5.2. Medium-Power PV Device

The second test was performed using a medium-power PV device. The environmental conditions were very similar to the ones from the previous case. The module used for this test was the KC85TS from Kyocera. The device is composed by two strings in parallel ( $N_p = 2$ ) of 36 cells ( $N_s = 36$ ). For this test, measurements were taken on the roof of the same building from case A. It must be noted that the module was not brand new. Installation was performed circa five years before the measurements. Nevertheless, results achieved were very satisfactory despite the possible divergences between manufacturer data and the actual open circuit/short circuit/maximum power characteristics. The RMS error, using (9) is about 3.2% as can be seen from Figure 7.

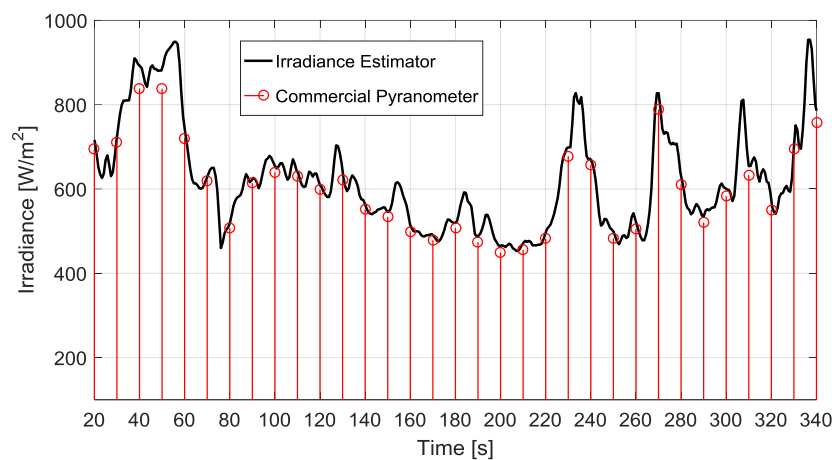


**Figure 7.** Irradiance profile predicted using a commercial pyranometer (red markers) and the proposed sensor on a medium power PV array. RMS is about 3.2%.

## 5.3. Neural Network-Based Pyranometer Comparison

The last test, reported in Table 2, shows the comparison of the prediction using the closed form herein proposed and the neural network-based estimator proposed in [8]. As can be seen, no error is reported, this is because the accuracy is very similar. Indeed, the neural network proposed in [8] reproduces the same functional relationship described in (9) by means of a numerical black-box model. The advantages of the closed forms can be seen clearly in terms of latency. The original neural network approach requires more computational resources with respect to the analytic approach herein proposed.

**Table 2.** Latency and memory footprint for neural network and closed-form-based sensors [8].

Profiling Figure	Neural Network	Closed Form
latency (clock cycles)	≈58,000	≈15,650
occupied Bytes	≈450	≈350
All. Bytes Static Random Access Memory (SRAM) (%)	≈0.99%	≈1.03%
computations/s	≈800	≈3000

## 6. Applications

The proposed approach can be useful both as a stand-alone instrument, and as an integrated measurement system for more complex control systems. Indeed, for a simple PV device, the setup proposed in Figure 3 is suitable for many purposes. The microcontroller samples voltage and current along with the digital acquisition of the temperature through the DS18B20 sensor. The irradiance information is computed through the irradiance expression on the MCU unit and can be used for

irradiance forecasting, fault detection and of course, Maximum Power Point Tracking. This tracking control requires the use of a programmable DC link able to exhibit a variable input resistance. A possible setup for this particular application is shown in Figure 8. Again, the MCU (denoted with the  $\mu$  letter) samples the voltage, the current and the temperature of the PV device. The device implements specific equations derived from the model to compute the MPP at specific  $G$  and  $T$ . The MPP in this case is represented by the optimal voltage  $v_{mpp}$  for the PV device. This voltage is used as input for a PI (proportional-integral) controller to tune the duty cycle (and by consequence, the input resistance/voltage) of the DC link. An accurate knowledge of the present irradiance makes it possible to compute the optimal work point for maximum power extraction. A very similar, yet less accurate approach can be pursued with suitably trained ANN. Irradiance sensing is also critical for larger power plants where environmental conditions may vary from panel to panel. In this case, the low cost of the proposed approach is very interesting since equipping every PV device in a plant with a dedicated commercial pyranometer can be economically unviable (Figure 9).

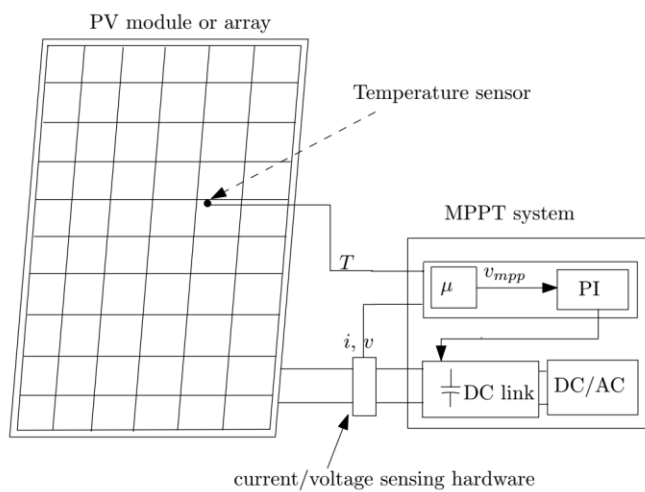


**Figure 8.** MPPT setup using a local irradiance sensor.

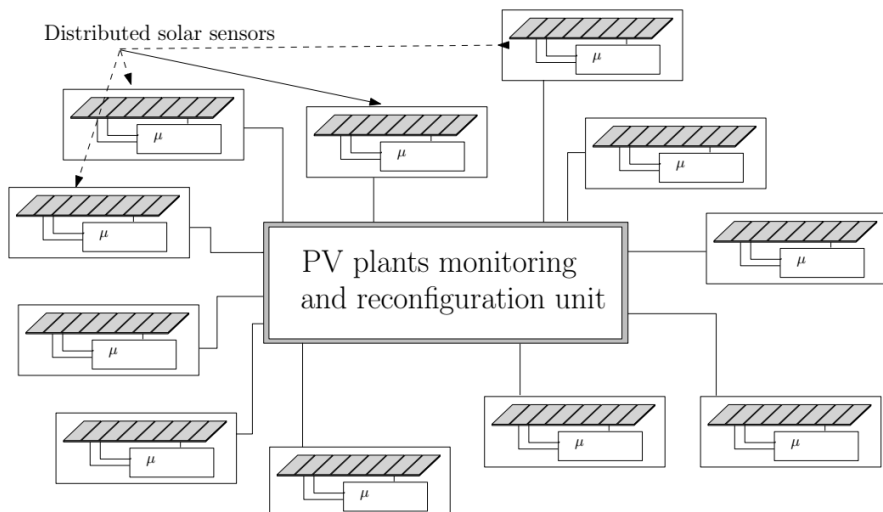


**Figure 9.** Distributed irradiance sensing for a reconfigurable PV plant.

## 7. Conclusions

This work analyzed the feasibility of solar irradiance assessment on a PV device assuming the knowledge of the device temperature, the voltage/current work point and the identified five

parameters model of the device. The approach was validated through different experiments, and the results obtained are comparable to the ones of a commercial instrument for irradiance sensing (pyranometer). The proposed approach has several advantages with respect to a pyranometer based measurement. First, the ease of implementation and the reduced costs makes this approach suitable for large-scale integration in a PV plant. Second, the possibility to use the power-producing PV device itself as a “sensor” solves all problems of alignment and spectral response, giving an irradiance estimation that is meaningful in terms of energy production (instead of a theoretical value, as the one given by commercial pyranometers). For temperature sensing, a back-mounted temperature sensor is sufficiently accurate for the evaluation. Moreover, it has the added benefit of being shaded by the panel itself for a more accurate measurement. Finally, the accuracy of the measurements obtained, the practical advantages of the implementation, and the reduced cost involved, make the approach proposed in this work especially important to address problems of partial shading, for which a local sensing of solar irradiance is a critical factor in maximizing the power output of the plant.

**Author Contributions:** Fernando Mancilla-David and Miguel Carrasco provided the experimental setup and the measurements. Alessandro Salvini, Francesco Riganti Fulginei and Antonino Laudani developed the analytic procedure to formulate the expression for irradiance. Gabriele Maria Lozito profiled the embedded implementation of the approach.

**Conflicts of Interest:** The authors declare no conflict of interest.

## References

1. Lave, M.; Reno, M.J.; Stein, J.; Smith, R. Low-cost solar variability sensors for ubiquitous deployment. In Proceedings of the IEEE 42nd Photovoltaic Specialist Conference (PVSC), New Orleans, LA, USA, 14–19 June 2015; pp. 1–6.
2. Velasco-Quesada, G.; Guinjoan-Gispert, F.; Pique-Lopez, R.; Roman-Lumbreras, M.; Conesa-Roca, A. Electrical PV array reconfiguration strategy for energy extraction improvement in grid-connected PV systems. *IEEE Trans. Ind. Electr.* **2009**, *56*, 4319–4331. [[CrossRef](#)]
3. Cristaldi, L.; Faifer, M.; Rossi, M.; Ponci, F. A simple photovoltaic panel model: Characterization procedure and evaluation of the role of environmental measurements. *IEEE Trans. Instrum. Meas.* **2012**, *61*, 2632–2641. [[CrossRef](#)]
4. Husain, N.; Zainal, N.; Singh, B.; Mohamed, N.; Mohd, N.N. Integrated PV based solar insolation measurement and performance monitoring system. In Proceedings of the 2011 IEEE Colloquium on Humanities, Science and Engineering (CHUSER), Penang, Malaysia, 5–6 December 2011; pp. 710–715.
5. Cruz-Colon, J.; Martinez-Mitjans, L.; Ortiz-Rivera, E. Design of a low cost irradiance meter using a photovoltaic panel. In Proceedings of the 2012 38th IEEE Photovoltaic Specialists Conference (PVSC), Austin, TX, USA, 3–8 June 2012; pp. 002911–002912.
6. Tan, R.; Tai, P.; Mok, V. Solar irradiance estimation based on photovoltaic module short circuit current measurement. In Proceedings of the 2013 IEEE International Conference on Smart Instrumentation, Measurement and Applications (ICSIMA), Kuala Lumpur, Malaysia, 25–27 November 2013; pp. 1–4.
7. Dunn, L.; Gostein, M.; Emery, K. Comparison of Pyranometers vs. PV reference cells for evaluation of PV array performance. In Proceedings of the 2012 38th IEEE Photovoltaic Specialists Conference (PVSC), Austin, TX, USA, 3–8 June 2012; pp. 002899–002904.
8. Mancilla-David, F.; Riganti Fulginei, F.; Laudani, A.; Salvini, A. A neural network-based low-cost solar irradiance sensor. *IEEE Trans. Instrum. Meas.* **2014**, *63*, 583–591. [[CrossRef](#)]
9. Laudani, A.; Riganti Fulginei, F.; Salvini, A.; Lozito, G.M.; Mancilla-David, F. Implementation of a neural MPPT algorithm on a low-cost 8-bit microcontroller. In Proceedings of the International Symposium on Power Electronics, Electrical Drives, Automation and Motion (SPEEDAM), Ischia, Italy, 8–20 June 2014; pp. 977–981.
10. Lozito, G.M.; Bozzoli, L.; Salvini, A. Microcontroller based maximum power point tracking through FCC and MLP neural networks. In Proceedings of the 2014 6th European Embedded Design in Education and Research Conference (EDERC), Milano, Italy, 11–12 September 2014; pp. 207–211.

11. Lozito, G.M.; Laudani, A.; Riganti Fulginei, F.; Salvini, A. FPGA implementations of feed forward neural network by using floating point hardware accelerators. *Adv. Electr. Electr. Eng.* **2014**, *12*, 30. [[CrossRef](#)]
12. Tian, H.; Mancilla-David, F.; Ellis, K.; Muljadi, E.; Jenkins, P. A cell-to-module-to-array detailed model for photovoltaic panels. *Sol. Energy* **2012**, *86*, 2695–2706. [[CrossRef](#)]
13. Soto, W.D.; Klein, S.; Beckman, W. Improvement and validation of a model for photovoltaic array performance. *Sol. Energy* **2006**, *80*, 78–88. [[CrossRef](#)]
14. Varshni, Y.P. Temperature dependence of the energy gap in semiconductors. *Physica* **1967**, *34*, 149–154. [[CrossRef](#)]
15. Palankovski, V. 3.3.1 Bandgap Energy. In *Simulation of Heterojunction Bipolar Transistors*; Institute for Microelectronics: Vienna, Austria, 2000; pp. 227–230. Available online: <http://www.iue.tuwien.ac.at/phd/palankovski/node37.html> (accessed on 01 March 2017).
16. Laudani, A.; Riganti fulginei, F.; Salvini, A. High performing extraction procedure for the one-diode model of a photovoltaic panel from experimental I–V curves by using reduced forms. *Sol. Energy* **2014**, *103*, 316–326. [[CrossRef](#)]
17. Laudani, A.; Riganti Fulginei, F.; Salvini, A. Identification of the one-diode model for photovoltaic modules from datasheet values. *Sol. Energy* **2014**, *108*, 432–446. [[CrossRef](#)]
18. Laudani, A.; Riganti Fulginei, F.; Salvini, A.; Lozito, G.M.; Coco, S. Very fast and accurate procedure for the characterization of photovoltaic panels from datasheet information. *Int. J. Photoenergy* **2014**, *2014*, 10. [[CrossRef](#)] [[PubMed](#)]
19. Da Costa, W.T.; Fardin, J.F.; De Vilhena, L.; Machado Neto, B.; Simonetti, D.S.L. Estimation of irradiance and temperature using photovoltaic modules. *Sol. Energy* **2014**, *110*, 132–138. [[CrossRef](#)]
20. Patnaik, B.; Mohod, J.; Duttagupta, S. Distributed multi-sensor network for real time monitoring of illumination states for a reconfigurable solar photovoltaic array. In Proceedings of the 2012 1st International Symposium on Physics and Technology of Sensors (ISPTS), Pune, India, 7–10 March 2012; pp. 106–109.
21. Rivera, E.; Peng, F. Algorithms to estimate the temperature and effective irradiance level over a photovoltaic module using the fixed point theorem. In Proceedings of the 37th IEEE Power Electronics Specialists Conference (PESC '06), Jeju, Korea, 18–22 June 2006; pp. 1–4.



© 2017 by the authors. Licensee MDPI, Basel, Switzerland. This article is an open access article distributed under the terms and conditions of the Creative Commons Attribution (CC BY) license (<http://creativecommons.org/licenses/by/4.0/>).